

Effect of Wet Steam on Aerodynamic Performance of Low-Pressure Exhaust Passage with Last Stage Blade

A. Q. Lin^{1†}, X. Y. Chang², L. H. Cao², H. Zhang¹ and L. X. Sun³

¹ College of Power and Energy Engineering, Harbin Engineering University, Harbin 150001, China

² School of Energy and Power Engineering, Northeast Electric Power University, Jilin 132012, China

³ College of Nuclear Science and Technology, Harbin Engineering University, Harbin 150001, China

†Corresponding Author Email: linaqiang493@sina.com

(Received October 17, 2018; accepted February 6, 2019)

ABSTRACT

The condensation of wet steam has important effects on the behavior of the flow field. To evaluate the aerodynamic performance of exhaust passage influenced by wet steam phase change condensation, a numerical investigation was conducted. Taking a 600 MW steam turbine as an example with consideration of the wet steam from the last stage blade and the steam exhaust of the BFPT (boiler feed water pump turbine), the governing equations of wet steam two-phase flow were adopted by the Eulerian-Eulerian approach. Results show that the wetness in the stator domain increases gradually while the wetness in the rotor domain varies little on the pressure surface and is in small increment on the suction surface. The velocity uniformity can be improved at condenser throat outlet as the mass flow or wetness increases. Moreover, the trend to improve the aerodynamic performance of exhaust passage benefits from the improvement of wetness at the last stage blade inlet. Conversely, with the increment of wetness at the BFPT inlet, the static pressure recovery coefficient reduces by 5.8% and the total pressure loss coefficient increases by 2.4%, resulting in a reduction of aerodynamic performance of exhaust passage.

Keywords: Exhaust passage; Wet steam; Aerodynamic performance; Last stage blade.

NOMENCLATURE

BFPT	boiler feed water pump turbine	Steam3v	steam-phase fluid
C_{ps}	static pressure recovery coefficient	THA	steam turbine heat acceptance
C_{pt}	total pressure loss coefficient	v_a	area-weighted average velocity
DNS	Direct Numerical Simulation	v_m	mass-weighted average velocity
LP	low pressure	α	steam3l. mass fraction, <i>i.e.</i> , wetness
LSB	last stage blade	β	steam3v. mass fraction
	fluid	λ	velocity uniformity coefficient

1. INTRODUCTION

The exhaust passage, connected with the last stage blade (LSB) upstream and condenser downstream, is a twin low pressure (LP) exhaust hood in a 600 MW condensing steam turbine. It is mainly made up exhaust hood and condensing throat. Since the last stage blade works in two-phase condensing flow with wet steam, the wet steam directly flows from the LSB into exhaust passage. Entropy of the flow field increases during the non-equilibrium condensation due to the thermodynamic losses (Bagheri-Esfe *et al.* 2016b). Then, the condensation of superheated steam in the LSB has important effects on the behavior of the

flow field, which not only produces the additional loss due to a deviation from the on-design condition but also increases the stagnation pressure loss and total entropy generation to decrease the turbine efficiency (Bagheri-Esfe *et al.* 2016a). Although an increase in wetness can improve the flow field uniformity and reduce the aerodynamic resistance as wetness enhances, excessive steam humidity also increases the loss in the steam turbine and increases the water droplet erosion on the LSB (Starzmann *et al.* 2013, Grübel *et al.* 2015 and Ilieva 2017). For thermal transfer and vacuum in condenser caused by wet steam flow, it is valuable to investigate the aerodynamic performance of turbine exhaust passage affected by wet steam.

For recent years, researches on the aerodynamic performance of exhaust passage focus principally on the structure redesign in such aspects as the flow guide, guiding cone, and built-in guide device (Fan *et al.* 2007 and Burton *et al.* 2013). Among the common methods of providing flow characteristics in the exhaust passage are a full-scale model test (Lagun *et al.* 1984), scale-model experiment (Zhang *et al.* 2007 and Veerabathraswam *et al.* 2016), and numerical investigation (Yoon *et al.* 2002 and Mizumi *et al.* 2013). Although the flow field is more realistic and accurate from the first two approaches, more flow parameters are not measured under the restrictions of practical application. Hence, a promising technology to capture more details of flow characteristic is to employ a numerical simulation method.

The condensation loss and supersaturation loss directly influence the aerodynamic performance during the phase transition process of wet steam. Although the Direct Numerical Simulation (DNS) can be obtained the high-fidelity result for complex flow field (Ma *et al.* 2015 and Tryggvason *et al.* 2016), the Reynolds-averaged Navier-Stokes (RANS) simulation is widely used as two-phase flow solution. Based on RANS simulations, Chrigui (2005), Noori Rahim Abadi *et al.* (2017) and Lin (2018) smartly use multiphase flow simulation method to get actual flow properties by Eulerian-Lagrangian Approach. Simultaneously, the Eulerian/Eulerian model is also used to simulate two-phase flow (White, 2003 and Gerber *et al.* 2004). For the numerical investigation of flow mechanism in wet steam turbine stages, more researchers on the process of droplet growth as the non-equilibrium condensation flow of wet steam could reflect the change of the nucleation rate of the liquid phase, droplet number and the radius of the droplet (Yu *et al.* 2015). However, when the steam flow is under the saturation line for the flow process of wet steam in the LSB, the condensation change of wet steam is in the Wilson points downstream (Wu *et al.* 2007). Due to condensation flow of wet steam to maintain near the thermodynamic equilibrium state, the wet steam flow in the LSB could be regarded as the phase translation process of the thermodynamic equilibrium. By applying to this assumption, Zhang *et al.* (2008) have presented the wet steam flow. They found that the wet steam could decrease the flow resistance and improve the flow uniformity in the exhaust passage when the thermodynamic behavior of wet steam was taken into account. Furthermore, Cao *et al.* (2017) found that different swirl strength, wetness, and the inlet air angle of exhaust hood influenced the aerodynamic performance at a great extent. The rotor tip clearance easily affected the steam turbine efficiency (Jang *et al.* 2015). So, it is necessary that the last stage blade and blade tip clearance leakage are considered into the numerical computational domain to be more real reflect the flow status in the exhaust passage (Musch *et al.* 2011 and Burton *et al.* 2014).

The previous researches on wet steam in the LP exhaust passage of steam turbine mainly consider

the wetness from the LSB but the wetness from the steam exhaust of the BFPT is not considered. As a continuous work, this paper performs a numerical calculation on wet steam flow in a twin exhaust passage of steam turbine. The flow characteristics in exhaust passage affected by wet steam from both the last stage blade and the steam exhaust of the BFPT are considered. Additionally, based on the coordinate of Eulerian to build the numerical model, the flow field of exhaust passage coupled with last stage blades is solved by the finite volume method. The changing characteristics of aerodynamic performance in exhaust passage are discussed at different wetness.

2. NUMERICAL MODEL

2.1 Geometric Configuration and Physical Model

The structure diagram of the typical LP exhaust hood in a 600 MW supercritical large power steam turbine is shown in Fig. 1. According to actual structure sizes in equal proportion, the twin LP exhaust passage connected last stage blade is illustrated in Fig. 2 in simplification. Computation domains mainly include the last stage blade, the steam exhaust of BFPT, inner steam extraction pipeline, and the LP heater, etc. The LSB is designed as 80 rotor blades and 52 stator blades. The radial height of the rotor blade and blade tip clearance are 1029 mm and 11.2 mm, respectively.

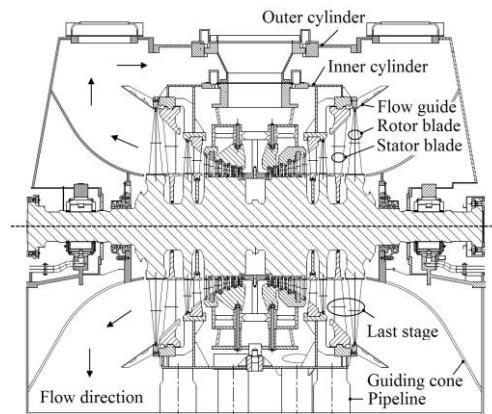
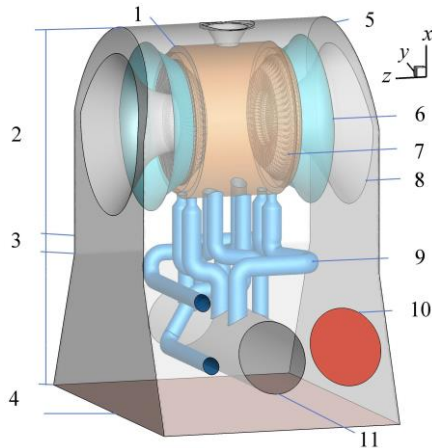


Fig. 1. Schematic diagram of the typical twin LP exhaust hood in a 600 MW steam turbine.

The model geometry is meshed using the ICEM CFD 17.0 software. The computational domain of last stage blade is discretized by the multiblock and structured grids to decrease the cells number, as shown in Fig. 3. And, the complex geometry model of exhaust passage is created by unstructured meshes to improve the quality of the grids. The first point near the wall boundary is located at the viscous sub-layer. To meet the requirements of the turbulence model of grid scale, the first layer of cell size is about 1×10^{-5} m in the last stage blade so that the dimensionless wall distance y^+ is less than 1, and the y^+ value for the exhaust passage domain is more than 30. There are about 12.16 million

computation grid cells with about 8.64 million in the positive and negative arrangement of last stage blade and 3.52 million in the exhaust hood.



1. LP inner cylinder; 2. Exhaust hood; 3. Expansion joint; 4. Condenser throat outlet; 5. LP outer cylinder; 6. Flow Guide; 7. Last stage; 8. Guiding cone; 9. Steam extraction pipeline; 10. Steam exhaust inlet of BFPT; 11. LP heater.
Fig. 2. Computational domain of the LP exhaust passage coupled with the last stage blades.

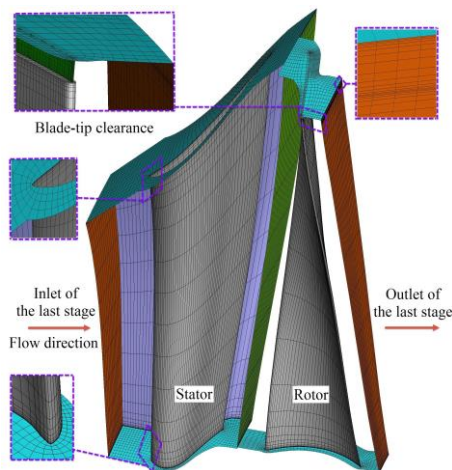


Fig. 3. Calculation Mesh of a passage in the last stage blade.

The partial differential equations controlling the flow field of exhaust passage are solved through commercial CFD simulator CFX 17.0. The iteration method is high order hybrid difference scheme. The standard $k-\epsilon$ turbulence model is adopted to solve the Navier-Stokes equations, and the flow region on low Reynolds number near the wall is conducted the wall function method of Salable to capture more detailed flow phenomenon. Moreover, the interface technology on numerical transfer between rotating and stationary computational domains are applied to the Stage model. In order to obtain a better solution result, the working fluid uses wet steam selected Steam3vl model in the IAPWS-IF97 library which can reflect the wet steam two-phase condensing flow including the steam-phase fluid (Steam3v) and liquid-phase fluid (Steam3l). The flow parameters are taken from the steam turbine heat acceptance

(*i.e.*, THA) which is typical steam turbine operating condition as shown in Table 1. Table 1 shows the inlet boundary data of computational domain at 100% THA.

With intention of decreasing the errors of numerical simulation, the calculation accuracy and validation method are qualified through comparing between scale-model experiment and numerical procedure as shown in the literature (Veerabathraswamy and Senthil, 2016) which focus to investigate turbulence model on the computational stability and the sensitivity of the inlet and outlet boundary condition types. They found that the difference in the predicted pressure coefficient on the diffuser and the outer casing is less than 6.2%. It is therefore that the mass flow is assigned to the inlet boundary condition and the computational domain outlet is set as the average static pressure of 4900 Pa. The convergence criteria of numerical accuracy are based on less than the levels of the order of 1×10^{-5} for the present study.

Table 1 Parameters on inlet boundary conditions at 100% THA

Inlet boundary	Last stage	BFPT
Flow rate/($\text{kg} \cdot \text{s}^{-1}$)	2×67.783	11.216
Total temperature/K	335.05	309.03
Wetness/%	5.5	4.7

2.2 Governing Equation

The exhaust steam out-flowing from the last stage blade of LP steam turbine is generally a state of wet steam. To obtain a more accurate numerical result, the steam/liquid two-phase is taken into consideration as a working fluid in this simulation. The Eulerian-Lagrangian particle tracking technique is used to capture the droplet on size, number, and distribution in the flow field, while the Eulerian-Eulerian multiphase model is applied to acquire the wetness on size and distribution. However, the flow is usually more paid attention to the wetness instead of the droplet in the exhaust passage of the steam turbine. Thus, the Eulerian-Eulerian multiphase flowing technique is used to investigate wet steam, giving the hypothesis that steam/liquid two-phase is the homogeneous continuous medium. This method assumes that the steam is a continuous item in the governing equations and the discretization item for the liquid, which is suitable for engineering practice to investigate the aerodynamic performance of the exhaust passage. And the flow characteristics are presented on the wet steam flow with homogeneous condensation and the variation of aerodynamic performance in the exhaust passage. The following is the governing equations of wet steam flow, including the homogeneous medium multiphase model and equilibrium phase transition model.

2.2.1 Homogeneous Medium Multiphase Model

The liquid-phase Steam3l and steam-phase Steam3v

are represented as α and β , respectively. The total number of phase is $N_p=2$. Hence, the subscript is a distinguished variable parameter of each phase, such as the volume fraction r_1 (r_2) which denotes the ratio of liquid-phase α (β) to the infinitesimal volume V . And, the conservation equation of volume for liquid- or steam- phase is given by:

$$V_i = r_i \cdot V, \sum_{i=1}^{N_p} r_i = 1, i=1, 2 \quad (1)$$

The density of phase α and β is ρ_1 and ρ_2 , respectively. The density of wet steam can be formulated as below.

$$\rho = \sum_{i=1}^{N_p} \rho_i r_i \quad (2)$$

The total pressure of wet steam can be obtained from the following equation.

$$p_{tot} = p_{stat} + \sum_{i=1}^{N_p} \frac{1}{2} \rho_i r_i U_i^2 \quad (3)$$

where, p_{stat} is the static pressure of wet steam, U_i is the velocity of liquid-phase ($i=1$) or steam-phase ($i=2$).

There is no slip between liquid-phase and steam-phase according to the assumption above, *i.e.*, the velocity U of wet steam is equal to that of each phase. The velocity U_i can be defined by:

$$U_i = U, (1 \leq i \leq N_p) \quad (4)$$

The mass conservation equation of the continuous phase (*i.e.*, steam-phase) can be written as the following formula.

$$\frac{\partial}{\partial t} (r_\beta \rho_\beta) + \nabla \cdot (r_\beta \rho_\beta U) = S_{MS, \beta} + M_\beta \quad (5)$$

where, $S_{MS, \beta}$ represents the mass source term. The mass source term M_β is the mass flow ratio transferring from the liquid-phase α to the steam-phase β .

The momentum conservation equation is calculated by:

$$\frac{\partial}{\partial t} (\rho U) + \nabla \cdot \{ \rho U U - \mu [\nabla U + (\nabla U)^T] \} = S_M - \nabla p \quad (6)$$

where, S_M is the momentum source term, μ is given as:

$$\mu = \sum_{i=1}^{N_p} \mu_i r_i \quad (7)$$

The energy conservation equation is expressed as:

$$\frac{\partial}{\partial t} (\rho H) - \frac{\partial p}{\partial t} + \nabla \cdot (\rho U H) = \nabla \cdot (\lambda \Delta T) + S_E \quad (8)$$

where, S_E the energy source term, H is given by the formula below:

$$H = h(p, T) + U^2 / 2 \quad (9)$$

To enclose the equations solved above, the constraint equation given constant pressure is presented in the following formula:

$$p_\alpha = p \quad (10)$$

2.2.2 Equilibrium Phase Transition Model

The equilibrium phase transition model is conducted, assuming what wet steam at saturation state is thermodynamic equilibrium. The phase transfer happens quickly so that the mass fraction for each phase of wet steam can be directly determined by the phase diagram. Thus, the Steam31 mass fraction can be expressed as

$$\alpha = \frac{h_{sat, v}(p) - h}{h_{sat, v}(p) - h_{sat, l}(p)} \quad (11)$$

where, h is static enthalpy, $h_{sat, l}$ and $h_{sat, v}$ are saturated enthalpy with the function of pressure for Steam31 and Steam3v, respectively.

2.3 Aerodynamic Performance Indicators

To evaluate the aerodynamic performance of exhaust passage with the change of local wet steam wetness, the uniformity coefficient is introduced to show the fluctuation degree of velocity, as following Eq. 12. Additionally, the uniform distribution of velocity at condenser throat outlet can be improved with increases of uniformity coefficient in favor of enlarging the thermal transfer of condenser.

$$\lambda = (1 - |v_m - v_a| / v_m) = v_a / v_m \quad (12)$$

where, v_a and v_m represent the area-weighted average velocity and the mass-weighted average velocity, respectively.

The aerodynamic performance on the conversion of leaving-velocity kinetic energy into pressure energy is defined as the static pressure recovery coefficient given by Eq. 13. Furthermore, the total pressure loss coefficient written by Eq. 14 is used for determining the degree of flow loss in the exhaust passage.

$$C_{ps} = (p_{s, 2} - p_{s, 1}) / (p_{t, 1} - p_{s, 1}) \quad (13)$$

$$C_{pt} = (p_{t, 1} - p_{t, 2}) / (p_{t, 1} - p_{s, 2}) \quad (14)$$

where, p_s and p_t are corresponding to the static pressure and total pressure, and the subscripts 1 and 2 represent on the inlet and outlet of the exhaust hood, respectively.

3. RESULTS AND DISCUSSION

3.1 Wet Steam Condensing Flow Analysis

Wet steam firstly flows into the stator blade, then accessing to the rotor blade and a partial to the blade tip clearance at a flow angle. In the end, the steam flow entries into exhaust passage with three-dimensional swirl flow. To a better understanding the influence of aerodynamic performance caused by the wet steam condensing phase transition, the flow characteristics in details is numerically investigated at 100% THA.

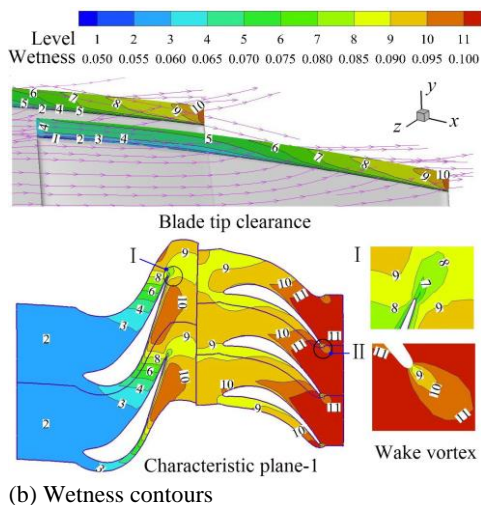
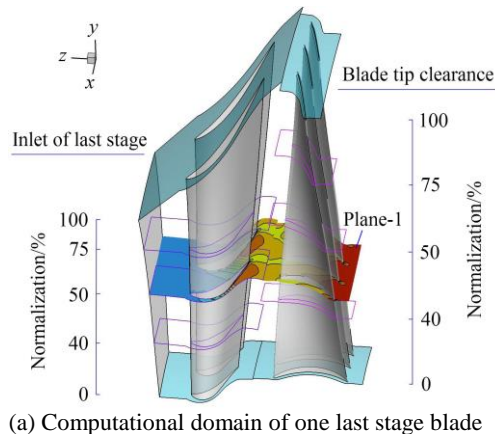


Fig. 4. Wetness distribution contours in the last stage passage.

The contour distributions of wetness among the last stage blade including the blade tip clearance are presented in Fig. 4. As shown in this figure, wetness on the middle of the pressure surface and the leading edge of the suction surface occurs a process of spontaneous condensation change. The trend of improving wetness in the stator blade cascades is about from 0.055 to 0.095; the wake region for wetness is in a small scope of 0.08 to 0.085. It is approximately at wetness value of 0.09 that wet steam flows into the rotor blade cascades in which the condensing phase change for wet steam is gradually started on the reality of the pressure surface and the

middle of the suction surface. A small range from 0.09 to 0.1 for wetness is in the wake region of the rotor blade, and the wetness of 0.1 is mainly focused at the outlet of the rotor blade. From the blade tip clearance can be seen that the wetness at the bottom is lower than that in the main flow region which wetness varies from 0.065 to 0.095 along the axial direction. One of the reasons to the phenomena mentioned above is that a part of wet steam fluid in the stator blade with an orientation inertial turns into the blade tip clearance, leading to what the rate of wet steam expansion in the blade tip clearance is less than that in the rotor blade domain so that the change of static pressure in the tip clearance is relative to small. In conclusion above, the scope of wet steam fluid condensing change in stator blade domain is much more than that in the rotor blade cascades. And a little of condensing phase transition for wet steam is in the high-speed area of the last stage blade. This is because the wet steam has not fully condensation in this region and then was forced to expand producing swirl flow and acceleration flow so that the rate of condensation change is lower in the rotor blade passages.

The contour distributions of pressure on the surface of Plane-1 are shown in Fig. 5 for the last stage blade. A comparison of the distribution between wetness and pressure is the one-to-one correspondence reflecting in what the wetness is related as a function of pressure, which the pressure value increases with decreases in the wetness region and vice versa. The pressure level reduces from Level-9 to Level-3 in stator blade while that decreases from Level-3 to Level-1 in rotor blade, which wet steam dropping pressure and acceleration process in stator blade passages is greater than that in rotor blade cascades. According to the larger range change of static pressure, the degree of liquid phase condensation for wet steam occurs obviously.

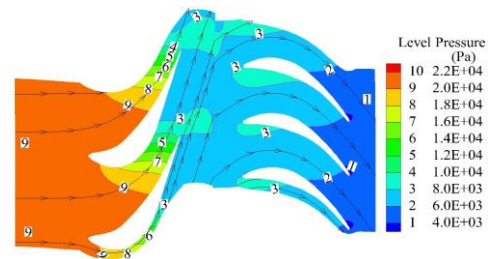


Fig. 5. Pressure contours of one last stage blade at plane-1.

The radial distribution of blade-surface wetness for a stator blade and a rotor blade are given in Figs. 6 and 7, respectively. The wetness along blade height is similar and varies slightly from 25% to 75% normalized span location. In the flow process through a blade row, wetness in the stator blade is gradually increased on both side of blade (*i.e.*, pressure surface and suction surface) with a downward trend at the region of the trailing edge (*i.e.*, the wake region); wetness in the rotor blade varies little on the pressure surface and is in small increment on the suction

surface with a downward trend at the wake region. Furthermore, on the stator blade (Fig. 6), the wetness at 25% span location varies from about 0.055 at the leading point to about 0.074 at the trailing point with a peak of about 0.088 near 96-percent pressure surface (*i.e.*, the wake region); the wetness gradually decreases along blade height from 25% to 75% mainly focusing on the latter part of the blade surface. On the rotor blade (Fig. 7), the wetness at 50% span location for pressure surface is larger than that for the suction surface. To the above-mentioned phenomena, the reason is that pressure on the pressure surface is more than that on the suction surface, resulting in what the pressure surface humidity is relatively small.

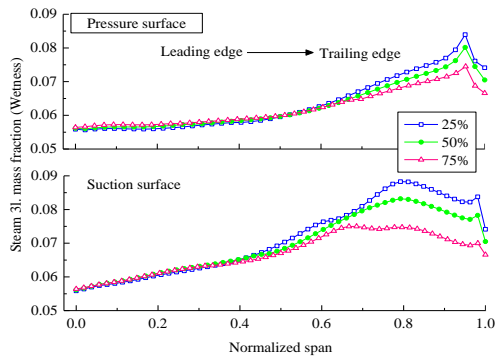


Fig. 6. Wetness distribution of a stator blade from 25% to 75% along with the normalization height.

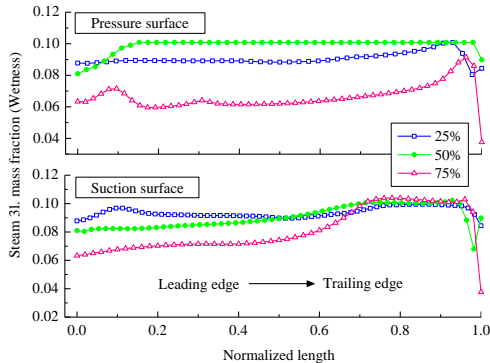


Fig. 7. Wetness distribution of a rotor blade from 25% to 75% along with the normalization height.

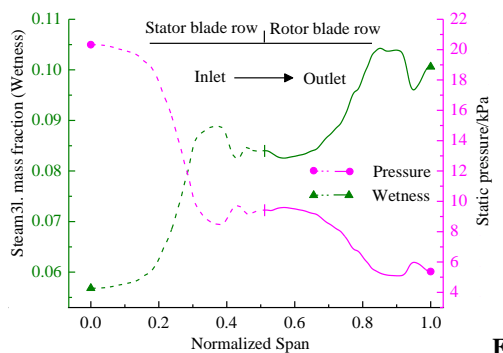


Fig. 8. A trajectory flowing from the inlet into outlet for the last stage blade.

The investigation of a tracing line for wet steam leads to the understanding of flow characteristics. Fig. 8 shows a target trajectory flowing from inlet to outlet within the last stage blade to analyze static pressure and liquid-phase mass fraction. The trend to wetness (*i.e.*, steam31. mass fraction) increases with decreases in static pressure along the flow direction. When wet steam goes into the blade cascades, the rangeability of wetness and static pressure are relatively large and that both parameters' changes are relatively flat at the inlet/outlet of the stator blade and rotor blade. For static pressure, a larger declining trend is made in the stator blade while a slow drop in the rotor blade, which is one reason that the rotor blade with high-speed rotation can be taken away the flow temperature to decrease thermal transfer in the rotor blade.

The flow parameters trajectory flowing from the inlet of the stator blade to outlet of the blade tip clearance are presented in Fig. 9. In this figure, the wetness and static pressure are both shown a small sinusoidal oscillation between the outlet in stator blade and the inlet in rotor blade, then the wetness gradually increases from 0.058 to 0.104 with decreases from 15.975 to 4.185 kPa for pressure in the rotor blade cascades. Nevertheless, the wetness plummets to 0.084 and pressure exists a small recovery after wet steam flow into the blade tip clearance. This can be seen from the comparing between Fig. 8 and Fig. 9 that the drop range of wetness in blade tip clearance is lower than that in rotor blade domain.

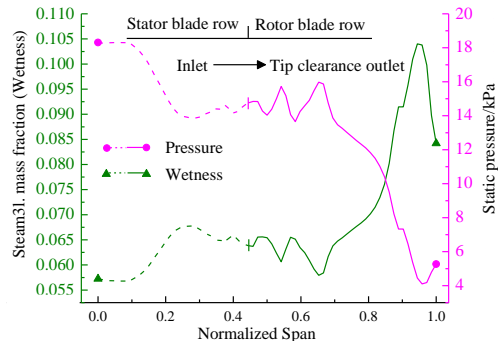


Fig. 9. A flow trajectory flowing from the inlet of the last stage blade into the outlet of the blade tip.

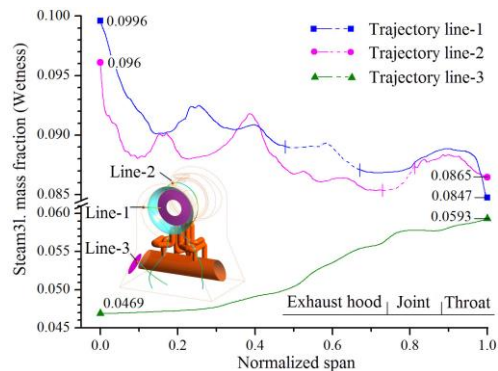


Fig. 10. Limited trajectory lines within the exhaust passage.

The marked changes for wetness in the exhaust passage are given by several different traced line as shown in Fig. 10. The liquid-phase mass fraction gradually decreases at the traced line-1 and line-2 presenting which the rangeability of wetness in exhaust hood is larger than that in condenser throat. This is mainly due to the wetness decreases with increases for the static pressure, thus gradually rising trends of static pressure in exhaust passage as a whole. On the other hand, when pressure loss caused by the impingement of between the BFPT flow and the upstream flow is presented, the wetness of the traced line-3 increases from 4.69% to 5.93%, which flow from the BFPT inlet to condenser throat outlet.

A comparison of the results evaluated performance for the computational domain of exhaust passage coupled with the last stage blade are shown in Table 2. The rangeability of wetness drop is around 0.025 in the stator blade, accounting for 61% in the whole of the last stage blade and which is greater than that about 0.016 in the rotor blade. In addition, the static pressure of exhaust passage increases by 88 Pa and the liquid-phase mass fraction in exhaust passage decreases by 0.013 caused by the effect of static pressure recovery. However, the range of static pressure in exhaust hood is 1.91 times in the exhaust passage and the wetness drop accounts for 69% of the exhaust passage. For the rangeability of total temperature in the flow field, the total temperature drop is only 2.72 K in exhaust passage while that is 25.24 K in the last stage blade domain. It is concluded that the aerodynamic performance of the exhaust hood can be evaluated that of the whole exhaust passage.

Table 2 Evaluated indicators on the aerodynamic performance of flow field

Computational domain	Pressure drop/kPa	Wetness drop	Temperature drop/K
Stator blade	9.936	-0.025	2.681
Rotor blade	5.216	-0.016	22.56
Last stage	15.152	-0.041	25.24
Exhaust hood	-0.168	0.071	1.88
Exhaust passage	-0.088	0.013	2.72

3.2 Aerodynamic Performance Analysis

Although the wet steam at the wetness of 0.10 and above is not allowed under actual operation for the last stage blade of LP steam turbine. In order to a better understanding of the aerodynamic performance in exhaust passage influenced by wet steam, the different wetness values are given through the inlet boundary condition under the 100% THA, as shown in Fig. 11. With the liquid phase mass fraction of wet steam increasing from 0.055 to 0.2 at the inlet of the last stage blade, the static pressure recovery coefficient increases from 16.01% to 23.41%. However, the total pressure loss coefficient of exhaust hood decreases from 56.22% to 50.89%. Thus, it can be seen that the aerodynamic performance of exhaust passage is

markedly improved while the inflow wetness from the last stage blade inlet is augmented, reducing total pressure loss and improving the ability of static pressure recovery. In turn, the efficiency of LP steam turbine would decrease because larger wetness could be produced more water droplet erosion on the blade surface.

Fig. 12 shows a change of aerodynamic performance for just increasing the inlet wetness of the BFPT under unchanging the inflow mass flow and inlet wetness of the last stage blade. With an increment of wetness at the BFPT inlet from 0.047 to 0.2, the aerodynamic performance evaluated indexes decrease by 5.8% and 2.4%, respectively, for the static pressure recovery coefficient and the total pressure loss coefficient, implying to decrease the aerodynamic performance of exhaust passage. Moreover, the changing phenomena above trend to be constant when the wetness is more than 0.1.

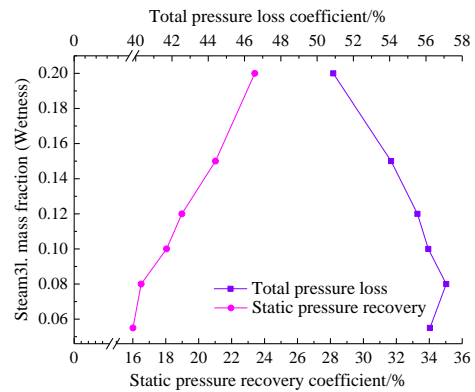


Fig. 11. Aerodynamic performance at different inlet wetness of the last stage blade under the same THA.

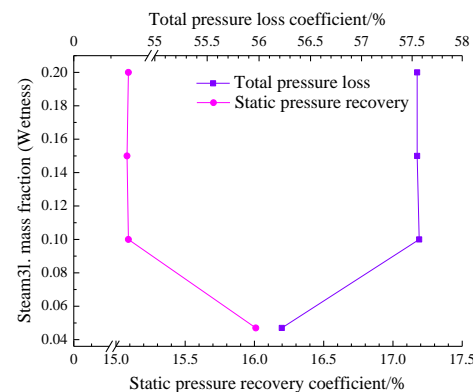


Fig. 12. Aerodynamic performance at different inlet wetness of the BFPT under the same THA.

A comparative study of the uniformity of velocity distribution under different inlet wetness between the last stage blade and the BFPT is carried out to find a changing trend as shown in Fig. 13. In this figure, for just changing the inlet wetness of the last stage blade at 100% THA, the velocity uniformity of condenser throat outlet increases from about 80.13% at the wetness of 0.06 to about 81.34% at the wetness of 0.20, which improves the

aerodynamic performance of exhaust passage. On the contrary, the uniformity coefficient is improved such wetness range as 0.047 to 0.10 for BFPT inlet wetness, while the inlet wetness of the BFPT in the range from 0.10 to 0.20 trends to a constant which does not impact on uniformity at an extent.

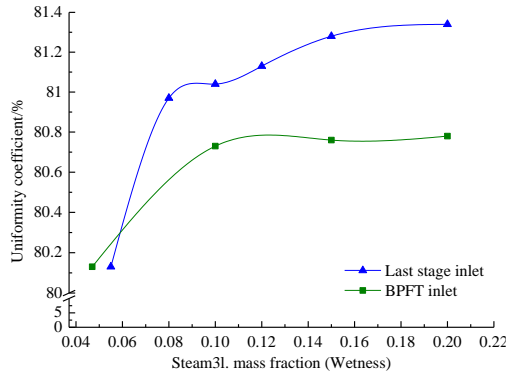


Fig. 13. Uniformity coefficient at different inlet wetness of the BFPT and last stage blade.

A tendency chart of aerodynamic performance affected by the variable working conditions presents in Fig. 14. The growth range of inlet wetness in BFPT varies from 0.009 to 0.047 and that of inlet wetness in last stage blade varies from 0.031 to 0.055 (*i.e.*, from 40% to 100% THA). In this figure, there are some differences and logical tendency in static- and total-pressure factors for different THA; its peak for the static pressure recovery coefficient is about 0.446 at the 50-percent THA and its minimum for the total pressure coefficient is about 0.55 at the 40-percent THA. The flow uniformity at throat outlet increases together with the increase of the wetness at the inlet from the last stage blade and the BFWT as the mass-weighted average velocity (*i.e.*, from the Eq. 12) decreases with increases of the liquid-phase mass fraction at the unchanged condition for mass flow and outlet area.

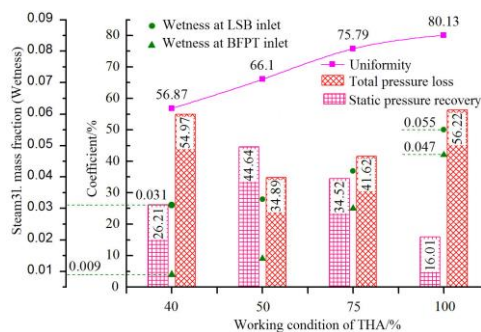


Fig. 14. Aerodynamic performance of exhaust passage at the different working condition of THA.

4. CONCLUSION

The numerical investigation is conducted to analyze the aerodynamic performance affected by the wet steam at different inlet wetness and typical LP

steam turbine operating conditions. The Eulerian-Eulerian multiphase model can be applied to simulate the flow field at the wetness of 0.10 and above. The calculation accuracy of numerical results is qualified by adopting the effective boundary conditions and turbulence model. Some of the conclusions can be drawn as follows.

The wetness in the stator domain is gradually increased on both the pressure surface and suction surface. Then, the wetness in the rotor domain varies little on the pressure surface and is in small increment on the suction surface. The higher condensing phase transition for wet steam can be found inside the stator domain compared with the rotor blade domains. Wetness is gradually increased in the last stage blade and steam exhaust of the BFPT while decreasing in the exhaust hood.

When the liquid mass fraction increases in the flow field of the LSB, the aerodynamic performance of exhaust passage becomes effective improved. However, with an increment of the BFPT inlet wetness, the static pressure recovery coefficient is declined by 5.8% and the total pressure loss increases by 2.4% so that the aerodynamic performance of exhaust passage is reduced.

ACKNOWLEDGMENTS

This work has been supported by the Ph.D. Student Research and Innovation Fund of the Fundamental Research Funds for the Central Universities (3072019GIP0304), which is gratefully acknowledged. Moreover, Aqiang Lin especially wishes to thank the help from his Master's supervisor Lihua Cao.

REFERENCES

Abadi Noori Rahim, S. M. A., A. Ahmadpour, S. M. N. R. Abadi and J. P. Meyer (2017). CFD-based shape optimization of steam turbine blade cascade in transonic two phase flows. *Applied Thermal Engineering* 112, 1575-1589.

Burton, Z., G. L. Ingram and S. Hogg (2013). A literature review of low pressure steam turbine exhaust hood and diffuser studies. *Journal of Engineering for Gas Turbines and Power* 135(6), 062001.

Burton, Z., G. L. Ingram and S. Hogg (2014). The influence of condenser pressure variation and tip leakage on low pressure steam turbine exhaust hood flows. *Proc. IMechE, Part A: Journal of Power and Energy* 228(4), 370-379.

Cao, L. H., H. Y. Si, A. Q. Lin, P. Li and Y. Li (2017). Multi-factor optimization study on aerodynamic performance of low-pressure exhaust passage in steam turbine. *Applied Thermal Engineering* 124, 224-231.

Chrigui, M. (2005). *Eulerian-Lagrangian approach for modeling and simulations of turbulent reactive multi-phase flows under gas turbine*

- combustor conditions*. PhD Thesis: Diss. Technische Universität.
- Bagheri-Esfe, H., M. J. Kermani and M. S. Avval (2016a). Effects of non-equilibrium condensation on deviation angle and performance losses in wet steam turbines. *Journal of Applied Fluid Mechanics* 9(4), 1627-1639.
- Bagheri-Esfe, H., M. J. Kermani and M. S. Avval (2016b). Numerical simulation of compressible two-phase condensing flows. *Journal of Applied Fluid Mechanics* 9(2), 867-876.
- Fan, T., Y. H. Xie, D. Zhang and B. Sun (2007, July). A combined numerical model and optimization for low pressure exhaust system in steam turbine. *ASME 2007 Power Conference*, San Antonio, USA, POWER2007-22147.
- Gerber, A. G. and M. J. Kermani (2004). A pressure based Eulerian/Eulerian multi-phase model for non-equilibrium condensation in transonic steam flow. *International Journal of Heat and Mass Transfer* 47(10-11), 2217-2231.
- Grübel, M., J. Starzmann, M. Schatz, T. Eberle, D. M. Vogt and F. Steverding (2015). Two-phase flow modeling and measurements in low-pressure turbines-Part I: Numerical validation of wet steam models and turbine modeling. *Journal of Engineering for Gas Turbines and Power* 137(4), 042602.
- Ilieva, G. (2017). Mechanisms of water droplets deposition on turbine blade surfaces and erosion wear effects. *Journal of Applied Fluid Mechanics* 10(2), 551-567.
- Jang, H. J., S. Y. Kang, J. J. Lee, T. S. Kim and S. J. Park (2015). Performance analysis of a multi-stage ultra-supercritical steam turbine using computational fluid dynamics. *Applied Thermal Engineering* 87, 352-361.
- Lagun, V. P., L. L. Simoyu, Y. V. Nakhman, V. A. Pakhomov (1984). Power characteristics of the exhaust of the modified low-pressure cylinder of the K-300-240 and K-800-240 turbines. *Thermal Engineering* 31(4), 26-32.
- Lin, A. Q., Y. G. Sun, H. Zhang, X. Lin, L. Yang and Q. Zheng (2018). Fluctuating characteristics of air-mist mixture flow with conjugate wall-film motion in a compressor of gas turbine. *Applied Thermal Engineering* 142, 779-792.
- Ma, M., J. C. Lu and G. Tryggvason (2015). Using statistical learning to close two-fluid multiphase flow equations for a simple bubbly system. *Physics of Fluids* 27(9), 092101.
- Mizumi, S. and K. Ishibashi (2013, June). Design philosophy and methodology of a low pressure exhaust hood for a large power steam turbine. *ASME Turbo Expo 2013: Turbine Technical Conference and Exposition*, San Antonio, USA, V05BT25A007.
- Musch, C., H. Stüer and G. Hermle (2011). Optimization strategy for a coupled design of the last stage and the successive diffuser in a low pressure steam turbine. *Journal of Turbomachinery* 135(1), 2407-2415.
- Starzmann, J., P. Kaluza, M. V. Casey and F. Sieverding (2013). On kinematic relaxation and deposition of water droplets in the last stages of low pressure steam turbines. *Journal of Turbomachinery* 136(7).
- Tryggvason, G., M. Ma and J. C. Lu (2016). DNS-assisted modeling of bubbly flows in vertical channels. *Nuclear Science and Engineering* 184(3), 312-320.
- Veerabathraswamy, K. and A. Senthil Kumar (2016). Effective boundary conditions and turbulence modeling for the analysis of steam turbine exhaust hood. *Applied Thermal Engineering* 103, 773-780.
- White, A. J. (2003). A comparison of modeling methods for polydispersed wet-steam flow. *International Journal for Numerical Methods in Engineering* 57(6), 819-834.
- Wu, Z. H., L. Li and Z. P. Feng (2007). Three-dimensional simulation of wet steam two-phase flows in the stator of a low-pressure turbine. *Journal of Engineering Thermophysics* 28(5), 763-765.
- Yoon, S, F. J. Stanislaus, T. Mokulys, G. Singh and M. Claridge (2011, June). A three-dimensional diffuser design for the retrofit of a low pressure turbine using in-house exhaust design system. *ASME 2011 Turbo Expo: Turbine Technical Conference and Exposition*, Vancouver, Canada, GT2011-45466.
- Yu, X. G., Z. H. Xiao, D. M. Xie, C. Wang and C. Wang (2015). A 3D method to evaluate moisture losses in a low pressure steam turbine: application to a last stage. *International Journal of Heat and Mass Transfer* 84, 642-652.
- Zhang, L. L., G. M. Cui, X. Guan and X. Z. Gao (2008). Condenser-throat flow simulation with due consideration of steam thermodynamic behavior. *Journal of Engineering for Thermal Energy and Power* 23(6), 572-576.
- Zhang, W., B. G. Paik, G. Y. Jang, S. J. Lee, S. E. Lee and J. H. Kim (2007). Particle image velocimetry measurements of the three-dimensional flow in an exhaust hood model of a low-pressure steam turbine. *Journal of Engineering for Gas Turbines and Power* 129(2), 411-419.